Influence of the ratio of drill bit size and conductor casing diameter on jetting with Lattice Boltzmann method

Anderson F. C. Gomes[1], Joyce K. F. Tenório[1], Beatriz R. Barboza[1], Eduardo M. A. Pacheco[2], João P. L. Santos[2], Fábio S. Cutrim[3], Rafael Dias[3]

[1]*Laboratory of Scientific Computing and Visualization, Federal University of Alagoas*
Av. Lourival Melo Mota, 57072-970, Alagoas/Maceió, Brazil
andersonfgomes@lccv.ufal.br, joyce.tenorio@lccv.ufal.br, beatriz@lccv.ufal.br
[2]*Center of Technology, Federal University of Alagoas*
Av. Lourival Melo Mota, 57072-970, Alagoas/Maceió, Brazil
eduardo.pacheco@ctec.ufal.br, joao.santos@ctec.ufal.br
[3]*Petrobras*
Av. Horácio Macedo, 21941-915, Rio de Janeiro/Rio de Janeiro, Brazil
fabiosawada@petrobras.com.br, rafael_dias@petrobras.com.br

Abstract. Conductor casing is the first stage of the wellbore. It is responsible for supporting the installation of the following strings by resisting the stresses involved in the entire process. The conductor seals unconsolidated formation and guarantees the ideal pressure balance between internal and external environments. Installation by jetting is a widely adopted solution in deep water due to its reduced execution time. Furthermore, the process requires attention to control the size of the cavity. This work presents a numerical simulation of the jetting in a clayey offshore soil during conductor casing placement, aiming to quantify the influence of the ratio between the drill bit and conductor diameters on soil disturbance and operation time and other operational parameters. A Lattice Boltzmann (LBM) model is adopted to deal with the soil-fluid interaction. A drill bit with three inclined nozzles rotates while jetting drilling fluid and descends alongside the jetting system toward the soil domain. The soil domain is governed by a viscoplastic model based on a Herschel–Bulkley fluid. The size of drill bit influences the soil area reached, allowing better control over the advance. The presented results help to properly understand the operational jetting parameters and can be employed to set optimal installation procedures.

Keywords: rheology, jetting, conductor casing.

1 Introduction

The conductor casing is the foundation in an oil well, the first structure to be installed, still in shallow soil. These first soil layers are poorly consolidated, so they offer minimal resistance to penetration. For excavations in such fragile layers, jetting emerges as a fast alternative. Wei et al. [1] suggested 300 kPa as the maximum soil shear strength to be seamlessly jetted.

The return on a well drilling investment is often uncertain and sensitive. The borehole installation must be well planned, and numerical simulations can provide an assessment of feasibility as well as optimizing the procedure. This paper is designed to provide a modelling methodology for the soil excavation step to prepare for installing the well foundation.

The mechanics of soil excavation during jetting presents considerable challenges [2]. In its more classical treatment, from a continuous element geomechanical perspective, large deformations lead to numerical errors that are extremely difficult to circumvent. Various strategies have been developed to deal with such complexities [3]. However, advances are still limited and do not embrace the need for a few tens of meters that the installation of a casing requires. This led some authors to the idea of treating the soil as a fluid, thus facilitating large deformations

without distortion problems.

In deeper environments, the ultra-deep marine soil usually presents itself as a cohesive clayey soil, in the form of a fine mud, and is thus a low-resistance material [4]. As this soil is composed mostly of clay-sized particles, these adhere tightly to each other, severely reducing the permeability of the assembly. Once the water penetrates the pores, it is hardly extracted, so this region is usually understood as a cohesive undrained soil [5]. Thus, a viable alternative is to approximate the modeling to a fluid-dynamic environment, admitting that the soil has the aspect of a mud, a fluid mass with reduced flow capacity with a, therefore, viscoplastic behavior [6].

Soil analysis by rheological approach is often adopted for landslides [7] [8], dam stability problems, retaining walls and marine landslides over pipes [9]. Another stream refers to soil excavation by dynamic deformation [10] [11] in which this work is inserted. Gupta and Pandya [12] demonstrated that undrained soils have behavior that range from elastic to viscous, and Vyalov [13] suggested Bingham's viscoplastic model, defined in eq. (1), to describe the behavior of soils under a stress state, where τ refers to shear stress, γ to the shear rate, μp is plastic viscosity and τy is the yield strength:

$$\begin{cases} \tau = \mu_p \gamma + \tau_y, \ for\ \tau > \tau_y, \\ \gamma = 0, \ for\ \tau \leq \tau_y. \end{cases} \tag{1}$$

This is because of the three-stage behavior described by Jeong [14] described in Fig. 1, where the first regime refers to the interactions of the soil particles under low shear, and therefore with the soil behaving as an elastic solid. The second step is the behaviour transition, where the strain rate reaches a critical value γc with onset of yield stress. Finally, the third regime becomes governed by viscosity, with the soil beginning to act as a fluid.

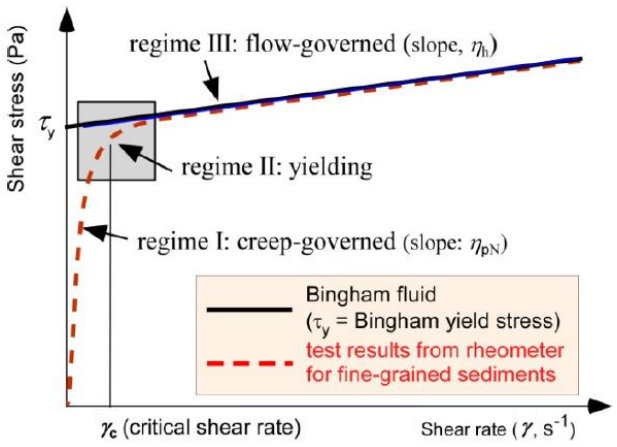

Figure 1. Flow behavior of fine-grained sediments. Source: Jeong [14]

The Bingham plastic model describes well fluids with low clay concentration, but higher concentrations lead to more pseudoplastic behavior [15]. Thus, to represent an undrained clay soil, a power fluid model with yield strength becomes more appropriate, such as the Herschel-Bulkley model defined in Eq. (2), where K is the consistency index and n is the behavior index:

$$\begin{cases} \tau = K \cdot \gamma^n + \tau_y, \ for\ \tau > \tau_y, \\ \gamma = 0, \ for\ \tau \leq \tau_y. \end{cases} \tag{2}$$

Both models tend to overestimate the actual yield strength since the plastic viscosity gradually decreases with strain rate. This leads to a discontinuity in the shear stress field so that both models become unable to describe the behavior of a fluid subjected to a shear stress below the yield strength (where the shear rate is zero) which are the rigid or non-shear stress zones [16]. Analyzing the equation, when the strain rate tends to zero, the viscosity tends to infinity, leading to the problem of discontinuous derivatives. Thus, some models for viscoplastic fluids arise as an alternative [17] [18]. Another possibility are modifications of the Herschel-Bulkley equation, a suggested modification is the one shown in Eq. (3), where a parameter μy referring to the yielding viscosity is included to stabilize the rigid stress zones [19]:

$$\tau = \begin{cases} \tau_y + K \cdot (\gamma^n - (\tau_y/\mu_y)^n), & for\ \tau > \tau_y, \\ \mu_y \cdot \gamma, & for\ \tau \leq \tau_y. \end{cases} \quad (3)$$

Given the fluid approach for soil, the excavation modeling of the soil in jetting is handled by computational fluid dynamics (CFD). Hence there are two possible approaches to the involved dynamics [20]: discrete and continuous. In the continuous approach (traditional in finite volumes and finite elements), the material is assumed to be a continuous environment at macroscopic scale while in the discrete approach used, based on the Lattice Boltzmann method (LBM), it is considered a mesoscopic system based on the momentum conservation of the collision between particles [21].

There is no direct discretization of the Navier Stokes equations in LBM. The material is represented as a set of moving particles carrying their properties and the method is aided by statistical tools [22]. According to Krüger et al. [20], the probability distribution is founded on a first stage with a set of particles fi moving from one node to its neighbor in the form x+eiΔt in a time step t+Δt and a second stage where the original particle at node i and the new particle interact and change their directions according to the stipulated by a collision operator Ωi. Thus, the set of velocity vectors generates the lattice for each node with the storage of the distribution function conforming to Eq. (4) where Fi represents an external force acting on the fluid as function of weights, specific mass, particle velocity, acceleration, and speed of sound and fieq is an equilibrium distribution function containing only macroscopic properties of the flow:

$$f_i(\vec{x} + \vec{e_i}\Delta t, t + \Delta t) - f_i(\vec{x}, t) = \Omega_{ij}\left[f_i(\vec{x}, t) - f_i^{eq}(\vec{x}, t)\right] + F_i \Delta t. \quad (4)$$

2 Methodology

The numerical model was developed in LBM-based software XFlow. The physical reference is the installation of a conductor casing by jetting in undrained clay soil. Since the soil resistance in the first meters is low, it is possible to consider the soil as a viscoplastic fluid with high viscosity and both the jetted water and soil are treated as immiscible fluids. The jetting system consists of the conductor casing, the drill string, and the drill bit. The entire jetting system is designed as rigid bodies consisting of shells, with dimensions as shown in Fig. 2.

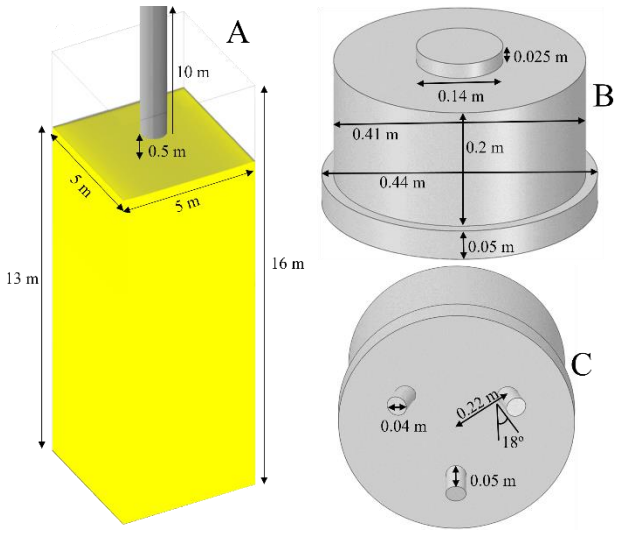

Figure 2. Numerical model dimensions with (A) all elements, (B) drill top view and (C) drill bottom view

The model was designed for a parametric analysis where three conditions are varied: the conductor and drill dimensions, the flow rate and drill rotation, Fig. 3 demonstrates the case studies. The dimensions shown in Fig. 2 refer to the 17.5-inch diameter drill bit (0.44 m). For the 14.75-inch (0.37 m) drill, the only modifications are the upper and lower diameters (which become 0.33 m and 0.37 m) while the positions of the nozzles are recentered. Some parameters were based on Akers [24].

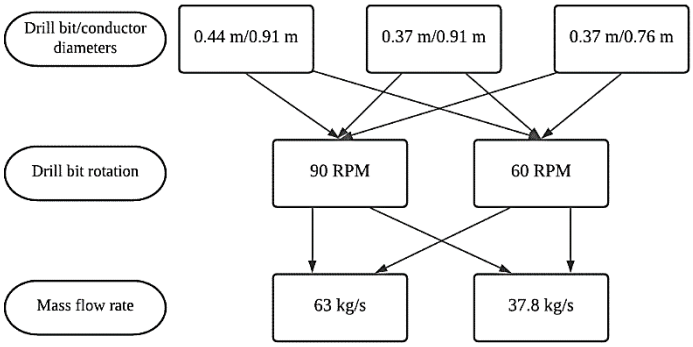

Figure 3. Studied values in parametric analysis

The whole domain is a rectangular cuboid with a width and length of 5 meters and a total height of 16 meters with 13 meters of soil and 3 meters of water. Water is also jetted through the drill nozzles at a constant flow rate while the drill rotates, and the entire system descends continuously at a rate of 25 cm per second. The nozzles are equidistant from each other and from center to edge and have 18° angle to the vertical axis. In addition to the 0.5-meter distance from the conductor to the mudline, the nozzles are 35 centimeters above the tip of the conductor for the larger drill and 25 cm on the smaller drill. The parameters of the fluids involved are given in Tab. 1. Water parameters were set at 20ºC and parameters for soil are given at Wang and Li [6] and Gomes et al. [25].

Table 1. Fluids involved parameters

Material	Soil	Water
Density (kg/m³)	2,300	998.3
Viscosity (Pa·s)		0.001
Yield stress (Pa)	30,000	
Consistency index (Pa·s)	216,960	
Flow index	0.1	
Yielding viscosity (Pa·s)	60,000	

The domain's sides and base are closed, while the top is open for material outflow. All solid walls have a free slip condition. Despite this condition hindering the conductor's adherence to the soil, an essential condition for stabilising the casing on soil, the interaction of the viscoplastic material with the conductor roughness was not well solved, leading to excessive material drag in other boundary conditions. The turbulence model adopted is based on a wall-adapting local eddy strategy that generalizes the turbulent viscosity to the smallest scales only and resolves higher scales.

3 Results and discussion

Parametric analyses were performed on 12 different models, as shown in Fig. 3, to evaluate the best scenario for the operating conditions involved. Besides operational aspects, using a viscoplastic model to model the soil is also a relevant aspect for discussion. Although it bypasses most numerical and physical problems of representing an undrained clay soil, the modified Herschel-Bulkley equation has four parameters without direct correlation to triaxial or other geomechanical tests.

The numerical problems of the classical Herschel-Bulkley model occur at low shear rates since the model becomes discontinuous. To overcome this problem, the value of the yielding viscosity that will represent the viscosity (and therefore the relationship between shear stress and shear rate) in the rigid stress zone can be pre-set. Yielding viscosity is the calculated viscosity at yield stress, i.e., the instantaneous slope found at the yield point of the rheological curve formed by shear stress and shear rate [26]. Yielding viscosity values vary significantly depending on the composition of the fluid, both the type of components (clay, xanthan gum, cement) and the concentration of each material in the fluid have an influence.

Qiu and Han [19] defined a proportional ratio of 1000x for yielding viscosity compared to yield stress when simulating concrete flow while the ratio was found experimentally by Prajapati and Ein-Mozaffari [26] was about

4x for concentrations of 1% xanthan gum in water. Considering the similarity of rheological behaviour between bentonite clays and xanthan, lower ratios were studied, leading to the definition of a doubled ratio.

3.1 Parametric analyses

Fig. 4 shows plan cuts at four different instants with volume fraction fields for the model with the largest drill bit, 90 RPM, and 37.8 kg/s flow rate to aid in understanding the procedure. The blue colour indicates the water, yellow field for the soil, and the jetting system in the centre consisting of the conductor, drill string and bit. At the beginning of jetting, the closest region to the mudline is widened larger than the conductor. This occurs due to the lower resistance of the soil in the region but is soon contained and the soil adheres to the pipe. Despite the free slip condition, with the descent of system, no external flow is perceived, which favours lateral resistance of the conductor..

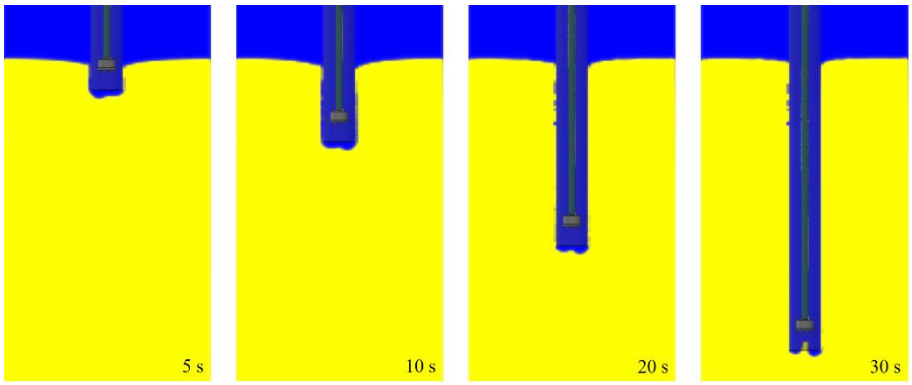

Figure 4. Volume fraction at different moments for 90 RPM and 37.8 kg/s in the system with a 0.44 m drill

The velocity needs to be sufficient to break through the soil. This soil breaking occurs when the kinetic energy exceeds the yield stress. Before this limit, no movement of soil occurs, and there is no excavation in the region. The jet velocity must exceed this reference value in the interfacial region. Once the jet leaves the nozzles, there is a loss of intensity due to the interaction with the static water. This loss intensifies with depth as pressure builds up due to the fluid column. The depths reached by jet depend strongly on the vertical position of the nozzles. Thus, Fig. 5 shows the relative position to the height of the nozzles for the four models with the largest drill bit. As already stated, the jetting system descends at a constant rate while the drill rotates as the modelling proceeds.

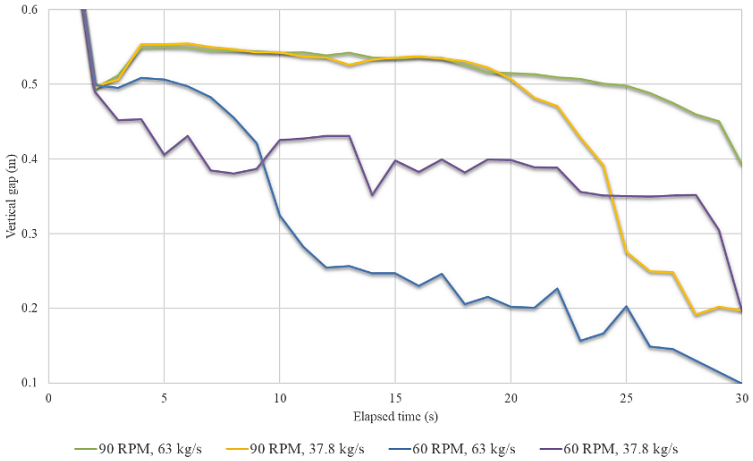

Figure 5. Nozzle spacing in rotation and flow rate variations for the 0.44 m drill over time

The scenario with the most linear consistency has the highest flow and rotation (green) since there is more

kinetic energy to keep digging the soil. This energy is also better applied due to the higher rotation. The two cases with lower rotations had rapid relative excavation loss since less radial dispersion of kinetic energy occurs; this, combined with the continuous descent of the system, causes less excavation of the soil, even with a similar flow. The scenario with higher rotation and lower mass flow (shown in Fig. 4) suffers considerable resistance around 25 seconds, mainly in the most central region, less reached by jets sloping outward. This suggests the need for a central nozzle or the action of the bits that were disregarded in this work formulation.

For the smallest drill bit (0.37 m diameter) with the largest conductor (0.91 m diameter) there is great difficulty for the jetting assembly advance, since it is a smaller drill bit responsible for a greatest excavation required. Significant amounts of soil entered the annular region, formed between the column and the conductor. This led to a two-phase annular, requiring a process of simultaneously driving the conductor into the soil. The higher-flow models advanced only to a depth of about 3 meters because soil resistance blocked the advance. This physical impediment occurred because the soil domain abutted the drill, numerically this meant extremely high-pressure values leading to divergence in the nozzles zone. The lower flow models were not even able to break through the first few centimeters of mudline, and since there was little advancement of the drills, there was no long-term glimpse of effects. All scenarios involving the 0.37/0.91 drill/driver ratio are plotted in Fig. 6.

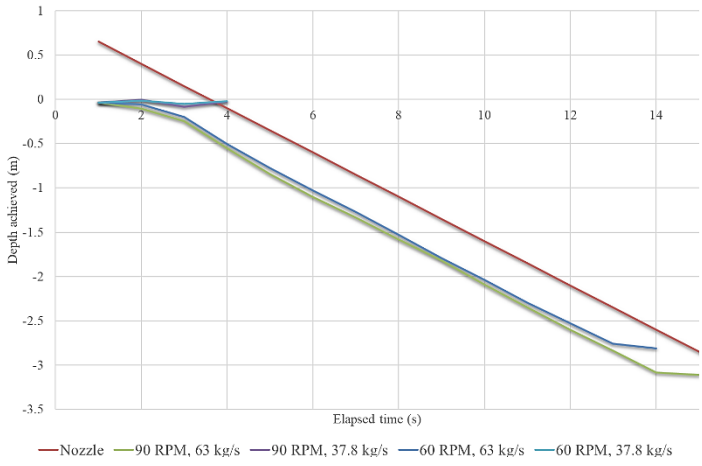

Figure 6. Nozzle spacing in rotation and flow variations for 0.37/0.91 ratio over time

For the models with smallest conductor the relative height of the drill bit to the conductor (bit stick-out) was reduced to avoid collision of the jet with the conductor. The soil remains invading the annular region, but with less intensity due to the smaller diameter required for the conductor. Physical obstruction also occurs around 3 meters for the higher flow models and near the mudline for lower flow rates.

4 Conclusions

According to previous studies, the defined parameters represented a sufficiently competent soil for a jetting. The viscoplastic formulation can faithfully portray a clay soil if combined with a geotechnical characterization of the environment. The flow rate of 37.8 kg/s was sufficient for the largest drill bit to advance into the soil with the conditions adopted for this study. The higher flow rate caused well break-in, reducing the healing capacity of the soil to adhere to the tube. Nevertheless, for the longer depths, the higher flow rate proved to be more appropriate. This leads us to believe that the best scenario is to start the jetting with lower flow rates and increase them according to the depth and, therefore, according to the increase of the natural resistance of the soil.

The smallest drills did not bring positive results for the studied soil. Thus, it is understood that they are only suitable for less resistant soils, regardless of the size of the conductor casing. Nevertheless, with higher flow rates it was possible to advance the jetting to a few meters in a stable manner even with partial driving. The rotation of the drill has a significant effect in extending and optimizing the radial area reached by the jets. Models with lower rotations suffered from greater resistance of the soil, leading to the assumption that for lower rotations it is necessary to reduce the descent speed of the system to allow earlier excavation. The intense activity of the water

with the soil led some models to suffer with soil crumbling in front of the auger. This raises the need for contingency measures such as increasing the flow rate or changing the rotation of the bit.

Acknowledgements. The authors would like to thank Petrobras for support given in the execution of this work.

Authorship statement. The authors hereby confirm that they are the sole liable persons responsible for the authorship of this work, and that all material that has been herein included as part of the present paper is either the property (and authorship) of the authors or has the permission of the owners to be included here.

References

[1] H. Wei, et al. "Study on Safety Control Technology of Surface Conductor Jetting Penetration in Ultra-Deep Water Soft Formation Drilling". In: *29th International Ocean and Polar Engineering Conference*, pp. 1435–1442, 2019.
[2] W. Meng, et al. "Simulation experiment and Mechanism Research on the Change of lateral friction against surface conductor in deepwater drilling". In: *Offshore Technology Conference*, 2016.
[3] D. Wang, et al. "Large deformation finite element analyses in geotechnical engineering". *Computers and Geotechnics*, vol. 65, pp. 104–114, 2015.
[4] L. R. Malouf. *Análise das operações de perfuração de poços terrestres e marítimos*. Graduation project, Federal University of Rio de Janeiro, 2013 [In Portuguese].
[5] N. Boukpeti, et al. "Strength of fine-grained soils at the solid-fluid transition". *Géotechnique*, vol. 62, n. 3, pp-213–226, 2012.
[6] T. Wang and H. Li. "Numerical simulation of jet excavation in conductor jetting operations". In: *Offshore Technology Conference*, 2014.
[7] D. F. M. Melo. *Comportamento reológico de solos sujeitos a corridas de lama por liquefação estática*. PhD thesis, University of São Paulo, 2014 [In Portuguese].
[8] M. Adamson. *Flow behaviour of fine-grained soils*. Master's thesis, Norwegian University of Science and Technology, 2017.
[9] G. Malgesini, et al. "Evaluation of debris flow impact on submarine pipelines". In: *Offshore Technology Conference*, 2018.
[10] H. Zhu and M. F. Randolph. "Numerical analysis of a cylinder moving through rate-dependent undrained soil". In: *Ocean Engineering*, vol. 38, n. 7, pp. 943-953, 2011.
[11] T. Wang and B. Song. "Study on Deepwater Conductor Jet Excavation Mechanism in Cohesive Soil". In: *Applied Ocean Research*, vol. 82, pp. 225-235, 2019.
[12] C. P. Gupta and A. C. Pandya. "Rheological Behavior of Soil Under Static Loading". In: *Transactions of the ASAE*, vol. 9, n. 5, pp. 718–724, 1966.
[13] S. S. Vyalov. *Rheological fundamentals of soil mechanics*. Elsevier Science Publishing Company, 1986.
[14] S. W. Jeong. "The effect of grain size on the viscosity and yield stress of fine-grained sediments". In: *Journal of Mountain Science*, vol. 11, n. 1, pp. 31–40, 2014.
[15] X. Huang and M. H. Garcia. "A herschel-bulkley model for mud flow down a slope". In: *Journal of fluid mechanics*, vol. 374, pp. 305–333, 1998.
[16] H. P. Soto. *Modelagem e simulação via formulações multicampos de Galerkin mínimo quadrados de escoamentos inerciais de fluidos de Bingham*. PhD thesis, Federal University Fluminense, 2010 [In Portuguese].
[17] T. C. Papanastasiou. "Flows of materials with yield". In: *Journal of Rheology*, vol. 31, n. 5, pp. 385–404, 1987.
[18] P. R. S. Mendes and E. S. Dutra. "Viscosity function for yield-stress liquids". In: *Applied Rheology*, vol. 14, n. 6, pp. 296–302, 2004.
[19] L. C. Qiu and Y. Han. "3d simulation of self-compacting concrete flow based on MRT-LBM". In: *Advances in Materials Science and Engineering*, vol. 2018, 2018.
[20] T. Krüger, et al. *The Lattice Boltzmann method*. Springer, 2017.
[21] A. A. Mohamad. *Lattice Boltzmann method*. Springer, 2011.
[22] J. G. Zhou. *Lattice Boltzmann methods for shallow water flows*. Springer, 2004
[23] C. Janßen and M. Krafczyk. "Free surface flow simulations on GPGPUs using the LBM". In: *Computers & Mathematics with Applications*, vol. 61.12 (2011), vol. 61, n. 12, pp. 3549-3563, 2011.
[24] T. J. Akers. "Jetting of structural casing in deepwater environments: job design and operational practices". In: *SPE Annual Technical Conference and Exhibition*, 2006.
[25] A. F. C. Gomes. "Análise paramétrica de jateamento de revestimento condutor em solo argiloso". In: *Rio Oil & Gas 2020 Technical Papers*, 2020. [In Portuguese]
[26] P. Prajapati and F. Ein-Mozaffari. "CFD Investigation of the Mixing of Yield-Pseudoplastic Fluids with Anchor Impellers". In: *Chemical Engineering & Technology*, vol. 32, n. 8, pp. 1211-1218, 2009.